6A.5 A GEOSPATIAL ANALYSIS OF RADAR REFLECTIVITY DATA FROM LANDFALLING TROPICAL CYCLONES

Corene J. Matyas *
University of Florida, Gainesville, Florida

1. INTRODUCTION

Tropical cyclones (TCs) can produce high rainfall totals that lead to flooding both near the coastline where fast winds and storm surges are also of concern, and hundreds of kilometers away from the location of landfall (Rappaport, 2000). The high rainfall rates produced by convective clouds can produce flooding rainfall in a relatively short amount of time (Geerts et al., 2000: Elsberry, 2002). Even though Hurricane Floyd (1999) was moving at a relatively fast forward velocity of 9 m s^{-1} during landfall, the high rain rates produced by convective processes caused more than 500 mm of rain to accumulate (Lawrence et al., 2001: Atallah and Bosart, 2003). Thus, it is important to identify the conditions under which convective clouds cover a large area within a TC's rain fields, and where these areas of convection exist relative to the circulation center.

Identifying spatial patterns in environmental data is a task for which a GIS is suited as the spatial characteristics of rainfall regions can be mathematically cataloged to facilitate comparisons. To better predict where a TC will produce the heaviest rainfall, the positions of convective rainfall regions must be determined relative to the circulation center of the TC as the system moves over land. The size of the convective rainfall regions and the speed of the storm are the two key variables required to estimate the duration of heavy rainfall in order to predict the total rainfall that a given location will receive.

This study employs a GIS to examine convective rainfall regions during the 24-hour period after TC landfall. Two research goals are pursued: 1) determine where regions of heavy rainfall exist in relation to the circulation center of the TC under different conditions, 2) determine the conditions under which the largest rainfall regions tend to form. To achieve these research goals, radar reflectivity returns are analyzed within a GIS to calculate the spatial properties of these regions as they relate to five factors. These factors are a) storm intensity, b) vertical wind shear, c) storm motion, d) whether or not a TC becomes extratropical, and e) distance from the coastline.

* *Corresponding author address:* Corene J. Matyas, Univ. of Florida, Dept. of Geography, Gainesville, FL 32611-7315; e-mail: matyas@ufl.edu

2. DATA

Radar reflectivity returns are obtained from the National Climatic Data Center's NEXRAD data archive (http://www.ncdc.noaa.gov/nexradinv/). Base reflectivity data from the Level III products are utilized when available. In cases where only the raw Level II data are available, data from the lowest scan elevation are utilized. For a TC to be analyzed in the current study, its rain fields must be within range of the radar for a 24-hour period after landfall. Thus, TCs that either dissipate within 24 hours of landfall (e.g., Matthew (2004)), or that did not remain over land for 24 consecutive hours after landfall (e.g., Charley (2004), Wilma (2005)) are not be included in the study. As a second U.S. landfall occurs for some TCs more than 24 hours after the first landfall, these subsequent landfalls are also analyzed. Overall, this study examines 43 U.S. landfalls from 38 TCs during 1995-2008.

The position of the circulation center at the time of landfall is taken from the National Hurricane Center (NHC)'s Hurricane Season Tropical Cyclone Report for each storm (http://www.nhc.noaa.gov/pastall.shtml). The time of landfall is rounded to the nearest half-hour. The position of the storm at all other analysis times, as well as its intensity as measured by the maximum sustained wind speed, and forward velocity and heading are obtained from the Hurricane best track database

(HURDAT) (NHC, 2006). A linear interpolation is performed to obtain data in three-hourly increments beginning at the time of landfall and ending 24 hours later. This process yields nine observation times for each TC landfall, or 387 total observation times for the 43 landfalls examined.

The velocity and direction of the vertical wind shear are acquired from the Statistical Hurricane Intensity Scheme (SHIPS) database (DeMaria and Kaplan, 1994: DeMaria et al., 2005). The vertical wind shear utilized is the difference between the 200 and 850 hPa winds calculated for an annular region located 200-800 km from the circulation center of each TC. The SHIPS data are also interpolated linearly to obtain data in the three-hourly time steps analyzed in this study.

3. ANALYSIS

The radar reflectivity data are first converted into a georeferenced format and imported into a GIS. Working with each three-hourly observation separately, the data from adjoining radars are combined into a single raster layer. A small amount of error is introduced into the analysis due to differences in calibration among the different radars and the range-dependent beam geometry and elevation (Anagnostou, 2004). At locations where multiple reflectivity values are available, the highest value is retained. Next, an interpolation is performed using inverse distance weighting to create contour lines in 5 dB*Z* increments that connect areas having the same reflectivity value. Once the contours are converted into polygons, spatial attributes are calculated for each polygon, including area and the latitude and longitude of the centroid, or center of mass.

As this study seeks to identify regions of heavy rainfall that may have the potential to produce flooding, only polygons larger than 500 km^2 in area that enclose reflectivity values of 40 dB*Z* or greater are retained. TC researchers such as Jorgensen (1984) have used 40 dB*Z* reflectivity values to denote heavy rainfall within convective rainbands. As shown in Figure 1, multiple convective regions of 40 dB*Z* reflectivity values over 500 km^2 in area may exist for a TC at a given observation time, and all such areas are analyzed in the current study.

Next, the attribute table of each convective polygon is expanded to include additional information relative to the five factors affecting convection for its observation time. Columns added to the attribute table include maximum sustained wind speed, direction and speed of vertical wind shear and storm motion, and the number of hours until the storm becomes extratropical, if applicable. The distance and bearing of each polygon centroid relative to the circulation center of the TC at each observation time is then calculated using spherical trigonometry. The positions of the polygon centroids are recalculated so that their bearings are in coordinates that are relative to the heading of the storm, and relative to the direction of the vertical wind shear. The GIS is also utilized to determine the distance from each polygon centroid to the nearest point on the U.S. coastline. In all, 21 columns of data exist for each convective region.

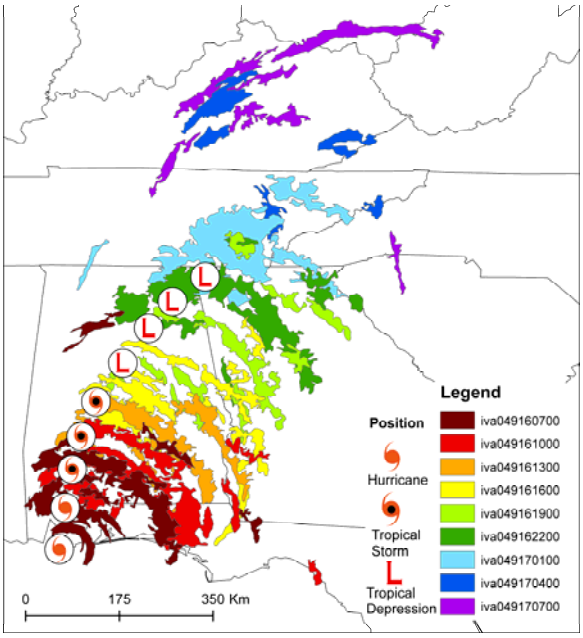

Figure 1. The 40 dB*Z* regions of Ivan (2004) greater than 500 km^2 in size every three hours from 0-24 hours post-landfall.

Two strategies are employed to determine which of the factors has the strongest association with the radial position of the convective regions relative to the circulation center of the TC. First, correlation coefficients are calculated between the distance of the convective region relative to the circulation center of the TC and the variables representing the six factors. As the data are not normally distributed, they are ranked from highest to lowest values and Spearman rank correlation coefficients (Wilks, 1995) are calculated.

The second strategy involves grouping the convective regions according to sub-classifications of each condition. Observations are grouped by the velocity of the maximum sustained winds: 1) greater than 33 m s^{-1}, 2) 17-33 m s^{-1}, or 3) less than 17 m s^{-1}. The regions are placed into one of three groups based on the speed of the vertical wind shear: 1) less than 5 m s^{-1}, 2) 5-10 m s^{-1}, or 3) greater than 10 m s^{-1}. This breakdown of slow, medium, and fast vertical wind shear is comparable to that of Corbosiero & Molinari (2002). These same divisions are used to group the convective regions according to the forward velocity of the TC. Four categories are developed to examine convection relative to the time that a TC becomes extratropical: 1) less than 24 hours, 2) 24-48 hours, 3) 48-72 hours, or 4) TCs that did not become extratropical within 72 hours of landfall. Distance relative to the coastline is divided into three categories: 1) more than 25 km offshore, 2) within 25 km of the coastline either on or offshore, or 3) more than 25 km inland. To examine the radial positions of the convective regions, the percent of observations in 100 km-wide annular rings extending outward from the circulation center is calculated for each condition-group. To characterize the azimuthal distribution of convection for each of the condition-groups, the percent of observations occurring in each quadrant of the storm is calculated.

To determine which of the five factors is most strongly associated with large areas of convection, a second dataset is constructed so that each observation time has only one entry. For each observation time, the areas of convective regions over 500 km^2 in size are summed. For this dataset, the distance from the coastline variable represents the distance of the circulation center of each TC from the nearest point on the coastline as calculated within the GIS. Spearman rank correlation coefficients are then calculated to determine if the largest areal extent of convection corresponds to the largest or smallest values of the five factors.

4. RESULTS AND DISCUSSION

The 43 TC landfalls examined in this study have 1545 regions of convection larger than 500 km^2 during the 387 observation times (Figure 2). On average, four convective polygons are present at each observation time, but 36 observation times contain no areas of convection larger than 500 km^2. Of the 43 landfalls examined, 25 occurred when the TC was a tropical storm rather than a hurricane. By twelve hours post-landfall, only Danny (1997) and Frances (2004) remained hurricanes, and most TCs were at tropical storm intensity. Therefore, the majority of convective polygons examined in the study occur when the TC is at tropical storm intensity. Also, in nearly half of the landfalls examined, TCs became extratropical within 72 hours of landfall.

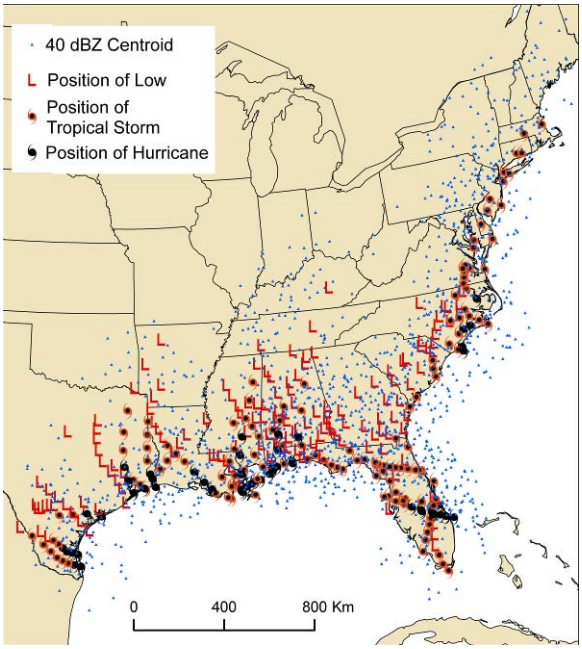

Figure 2. Locations of the position and intensity of each TC and the 40 dB*Z* region centroids.

4.1 Location of Convection Relative to Storm Center

Results suggest that the forward velocity of the TC has the largest effect on the location of convection both in the azimuthal and radial directions during the 24 hours after landfall. Overall, more convection occurs on the right side of the storm rather than the left (Figure 3), which agrees with the findings of previous research (Frank and Ritchie, 1999: Corbosiero and Molinari, 2003: Lonfat et al., 2004: Chen et al., 2006). Shapiro (1983) explains that storm motion induces asymmetries in the boundary layer frictional drag due to the stronger winds on the right side of the vortex that result when translation speed is added to the rotational speed of the tangential winds. The current study finds that in TCs moving at velocities under 5 m

s^{-1}, convection is evenly split between the right front and rear quadrants of the storm. When TCs are moving at 5-10 m s^{-1}, 60% of convective observations occur in the right front quadrant and only 21% are located in the rear of the storm. Almost 55% of convective observations for TCs with forward velocities exceeding 10 m s^{-1} occur in the left front quadrant, and 95% occur in the forward half of the storm, indicating a counterclockwise shift in the location of convection as forward velocity increases. This is similar to the pattern described by Kimball (2008).

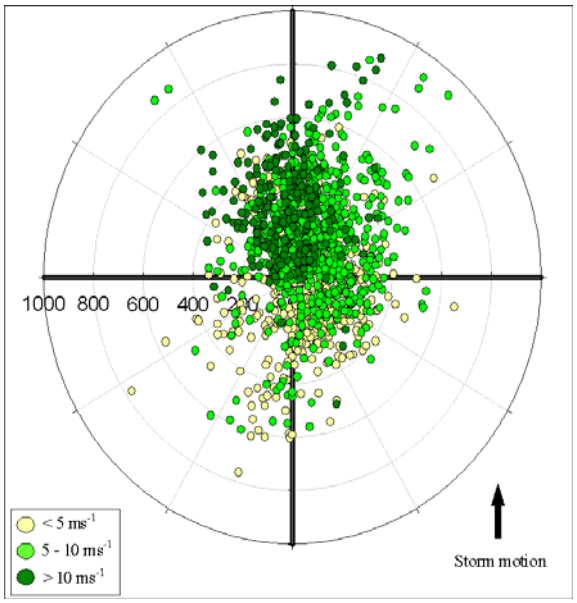

Figure 3. Centroids of convective regions placed according to the direction of storm motion and classified according to the speed of forward velocity.

Forward velocity is also important when considering the distance from the circulation center at which convection tends to occur. The correlation between centroid distance and storm forward velocity demonstrates that storm motion has the strongest association with the radial distribution of convection out of all six factors tested (Table 1). Among TCs with forward velocities below 5 m s^{-1} and 5-10 m s^{-1}, approximately 70-75% of observations occur within 300 km of the circulation center. However, 52% (17%) of observations in TCs moving at speeds greater than 10 m s^{-1} occur beyond 300 km (500 km). This has important implications for the findings of previous research as studies examining convection only within 400 km of the circulation center (e.g., Chen et al., 2006: Cecil, 2007) may have missed as much as one third of the convection associated with fast-moving TCs. Even more importantly, studies examining data within only 300 km of the circulation center (e.g., Molinari et al., 1999: Corbosiero and Molinari, 2002: Corbosiero and Molinari, 2003) may have missed more than half of the convection that exists in fast-moving TCs.

Table 1. Spearman Rank correlation coefficients for each convective region's centroid distance, and for the total areal extent of all convective regions at each observation time. Bold values are statistically significant at $\alpha = 0.01$.

Factor	**Centroid Distance** (n=1545)[a,b]	**Areal Extent** (n=387)[c]
Motion	**0.235**	**0.524**
Intensity	**-0.143**	**0.461**
Time until Extratropical	**-0.189**[a]	**0.274**
Shear	-0.057[b]	-0.018[c]
Distance to Coastline	0.034	0.013

[a] n = 908, [b] n = 1152, [c] n = 273

The number of hours until a TC becomes extratropical also exhibits an association with the location of convection in TCs after landfall (Figure 4). When a TC is within 48 hours of becoming extratropical, convection decreases markedly in the inner 100 km, while in the region of the storm beyond 300 km, the number of convective polygons increases to 43% of the total number of observations. These results suggest that a spreading out of convection occurs as a storm becomes extratropical. The negative correlation between centroid distance and hours until the TC becomes extratropical (Table 1) supports this finding.

Although the majority of the convective polygons remain in the right front quadrant regardless of when or if an extratropical transition happens, a shift in the counterclockwise direction towards the left front quadrant occurs as TCs approach the time that they become extratropical (Figure 4). At 48-72 hours before becoming extratropical, nearly 50 (25) % of convection is in the right front (rear) quadrant. Twenty-four hours later, the right front (rear) quadrant contains 61 (10) % of the convection, while the percentage of observations within left front quadrant increases only slightly. However, in the next 24 hours, the amount of convection in the right (left) front quadrant decreases (increases) to 49 (42)%,

completing the counterclockwise shift. Ritchie and Elsberry (2001) and Atallah and Bosart (2003) explain that this shift in the azimuthal location of convection occurs when relatively cool and dry air that diminishes convection advects counterclockwise around the circulation center beginning southwest of the TC. Meanwhile, convective precipitation is enhanced to the north of the circulation center as the warm and moist air of tropical origin on the eastern side of the TC is uplifted.

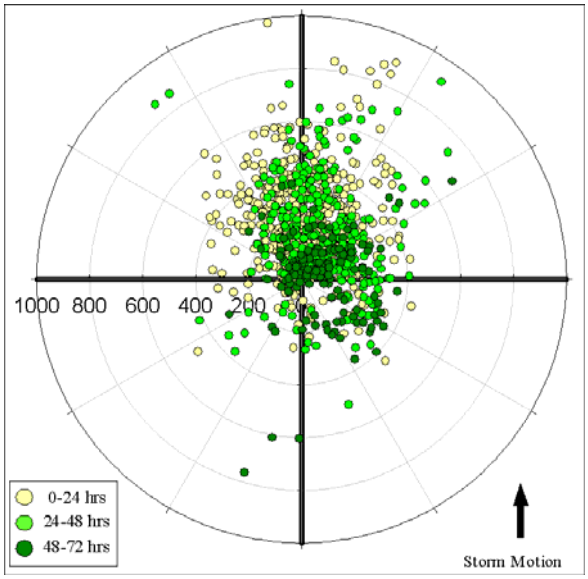

Figure 4. Centroids of convective regions placed according to the direction of storm motion and classified according to the time until completion of extratropical transition.

The speed of the vertical wind shear appears to exert a stronger influence on the azimuthal rather than the radial distribution of convection after landfall (Figure 5). When all observations are considered, most of the convection is located in the downshear left and right quadrants, which is in agreement with the findings of Corbosiero & Molinari (2002), Chen et al. (2006), and Cecil (2007). However, a clockwise shift in the position of the convective regions is observed as vertical wind shear increases. For TCs experiencing vertical wind shear speeds less than 5 m s^{-1}, 39 (28)% of the observations occur in the downshear (upshear) left quadrant. When the velocity of the vertical wind shear increases to 5-10 m s^{-1}, the number of observations increases (decreases) to 53 (17)% in the downshear (upshear) left quadrant. When strong vertical wind shear is present, only 6% of observations are located in both upshear quadrants, while 53 (36)% are located in the downshear left (right) quadrants. This clockwise shift in convection with increasing vertical wind shear has not been discussed by previous researchers. Figures from Corbosiero & Molinari's (2002) study only indicate that the downshear quadrants experience the most lightning flashes in both the inner 100 km and outer 100-300 km regions of the storm regardless of the strength of the vertical wind shear.

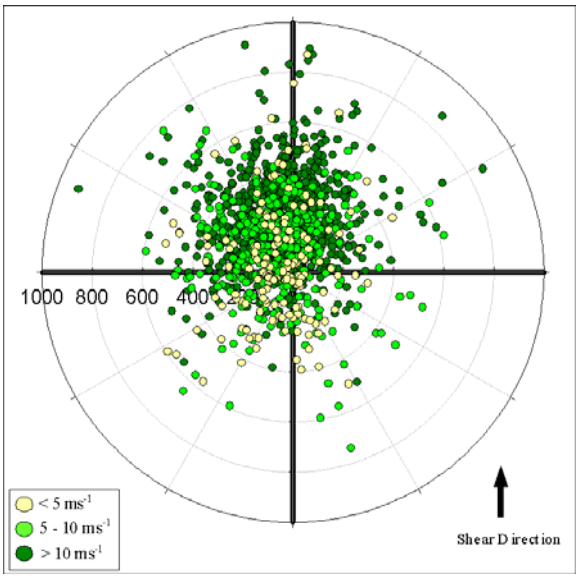

Figure 5. Centroids of convective regions placed according to the direction of the vertical wind shear and classified according to the velocity of the shear.

While the speed of the vertical wind shear appears to influence the azimuthal distribution of convection, it has a much weaker association with the radial distribution of convection as compared to storm motion. Approximately 30% of convective observations are located 100-200 km from the circulation center, and less than 20% are located in either the inner core, or beyond 400 km regardless of the velocity of the vertical wind shear. This suggests that stronger wind shear values do not result in the development or displacement of convection farther from the circulation center. The lack of a statistically significant correlation between the velocity of the vertical wind shear and the distance of the convective observations relative to the storm center (Table 1) supports this finding.

Convection is present in both the core and outer rainbands of hurricanes, while weaker TCs have little convection present within their core

(Figure 6). Hurricanes have nearly the same number of convective regions within 100 km of the circulation center as they do in the region 100-200 km from the circulation center where the edge of the principal rainband is often located (Willoughby et al., 1984: Molinari et al., 1999). Tropical storms have a clear maximum in convection 100-200 km from the circulation center. Twice as many convective observations are located 300-400 km from the circulation centers of tropical depressions than within the innermost 100 km, indicating a lack of convection near the core. The negative correlation coefficient between intensity and the distance of the observations from the circulation center indicates that higher intensity correlates to a closer centroid distance (Table 1). As the majority of the observations occur on the right side of the storm (Figure 6) in all three sub-groups, intensity does not appear have as strong of an association with the quadrant in which convection is located as does storm motion and vertical wind shear.

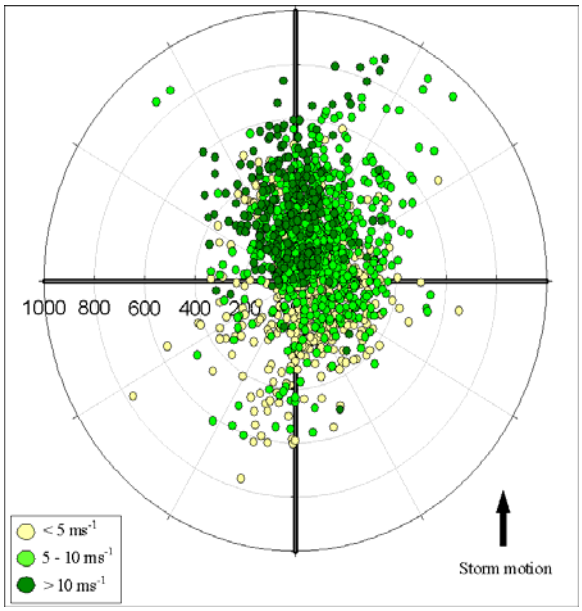

Figure 6. Centroids of convective regions placed according to the direction of storm motion and classified according to storm intensity.

The distance at which convection forms relative to the coastline appears to have some association with the azimuthal distribution of convection relative to the circulation center of the storm. Convection exists in the left rear quadrants of some TCs (Figure 7) despite this area being the most unfavorable location for the formation of convection given that downward vertical motion is enhanced on the left side of a TC (Powell, 1990). While many TCs track inland after landfall, some travel across the peninsula of Florida (e.g., Erin (1995)) or track parallel to the U.S. coastline (e.g., Hanna (2008)). Thus, convection located more than 25 km offshore may occur in any motion-relative quadrant of the storm. In this study, over 50% of the offshore convection is located in the rear quadrants of the TCs (Figure 7). The 45% of offshore observations located in the right front quadrant are associated with TCs making landfall along the east coast of the U.S. and moving towards the north. Offshore observations located the farthest from the circulation center in the right front quadrant exist in TCs that are nearing the time at which they become extratropical.

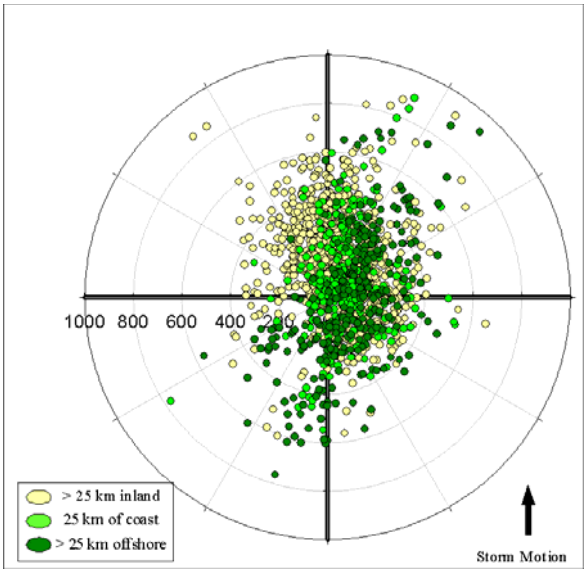

Figure 7. Centroids of convective regions placed according to the direction of storm motion and classified according to their distance from the coastline.

Results from the analysis of the near-shore observations suggest that the coastline does exert an influence on the azimuthal location of convection as TCs make landfall and move inland. Previous studies have discussed how frictional convergence produced along the coastline along the right side of the storm enhances the development of convection as a TC makes landfall (e.g., Jones, R. W., 1987: Frank and Ritchie, 1999). However, more than 35% of the observations occur in the two rear quadrants of the storm, suggesting that the coastline influences convective precipitation even after the circulation center has moved

inland. Additionally, since convection occurs near the coastline more than 300 km away from the circulation center, coastal areas not affected by the strongest winds in a landfalling TC may still experience heavy precipitation.

4.2 Areal Extent of Convection

The largest regions of convection are associated with fast-moving TCs that are nearing the time of transition to extratropical and located within 50 km of the coastline. Of these three factors, storm motion has the strongest relationship with the areal coverage of convection (Table 1). TCs that are moving at speeds exceeding 10 m s^{-1} have larger areas covered by convection on average than any of the other sub-groups examined. The nearly 30,000 km^2 average areal coverage of convection for fast-moving TCs is 20,000 km^2 more than for TCs moving at 5-10 m s^{-1}, and approximately 10,000 km^2 more than for TCs that are within 24 hours of becoming extratropical. The top ten largest convective areas occur in TCs with forward velocities greater than 8 m s^{-1}, and very few TCs that are moving at this speed have small areas of convection (Figure 8).

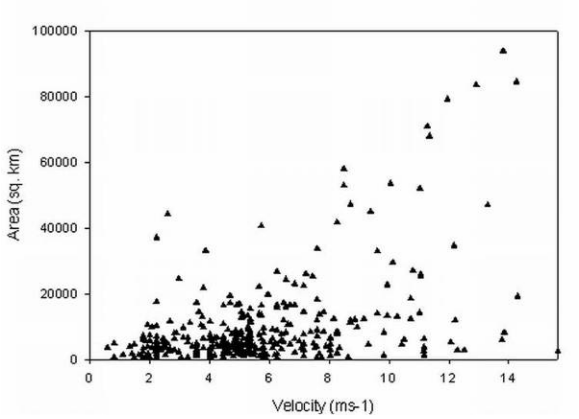

Figure 8. The areas of convective regions according to the forward velocity of the TC.

Interaction with a middle latitude trough causes storm motion to increase, and can also cause the TC to become extratropical (Jones, S. C. et al., 2003). All observation times that feature TCs moving at speeds greater than 10 m s^{-1} also occur when TCs are within 24 hours of becoming extratropical. However, all TCs within 24 hours of becoming extratropical do not necessarily move at fast forward velocities. Nearly 60% of the observations from this group occur when forward velocity is below 10 m s^{-1}. As a TC becomes extratropical, the surrounding environment becomes baroclinic and the isentropic ascent of the moist air mass associated with the TC enhances precipitation and causes the region within which heavy rainfall occurs to increase in area (Atallah and Bosart, 2003: Jones, S. C. et al., 2003). As a group, TCs that are within 24 hours of being extratropical have the second largest areas of convection on average. The ten largest areas of convection are associated with Floyd (1999), Hanna (2008), and Bertha (1996), which moved towards the north at speeds greater than 9 m s^{-1} as they transitioned into extratropical storms. The average area of convection increases for TCs as the time until their extratropical transition. The statistically significant correlation coefficient between areal extent of convection and time until becoming extratropical (Table 1) also supports the finding that extratropical transition results in larger regions of convection. For TCs that do not experience an extratropical transition, convection develops over an area of approximately 22,000 km^2 in the largest case (Figure 9), but convection is more commonly confined to an area measuring approximately 5000 km^2.

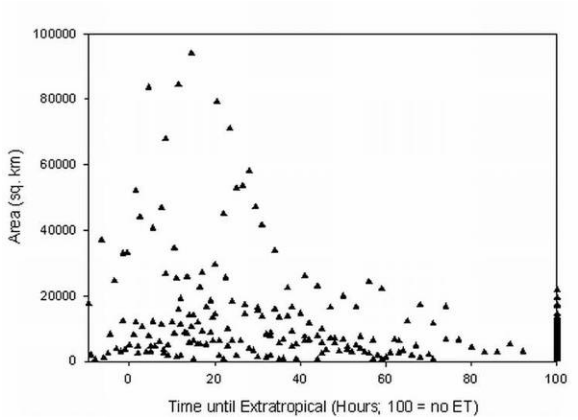

Figure 9. The areas of convective regions according to the time until extratropical transition. Observations along the 100 hour line are for TCs that did not become extratropical.

The second largest correlation with convective area is the maximum sustained wind speed (Table 1), indicating that the area covered by convection is largest for hurricanes and

decreases as TCs weaken. Although the five largest regions of convection belong to tropical storms (Figure 10), numerous regions smaller than 1000 km^2 exist for both tropical storms and tropical depressions. In hurricanes, however, the smallest region is more than 2100 km^2 in size. Hurricanes have convection in both their core and in their outer rainbands so that greater total area is covered by convective rainfall than for weaker TCs. This finding is consistent with that of Shepherd et al. (2007). Also contributing to the large spatial coverage of convection for hurricanes is their location close to the coastline. When the TC is located inland and the tangential winds are weaker, it is more difficult to advect moisture from the ocean into the circulation to sustain heavy rainfall (Bluestein and Hazen, 1989). The exception to the trend of diminishing convection as maximum sustained winds weaken after landfall occurs when TCs become extratropical. Many of these TCs are at tropical storm intensity as the size of their convective area grows.

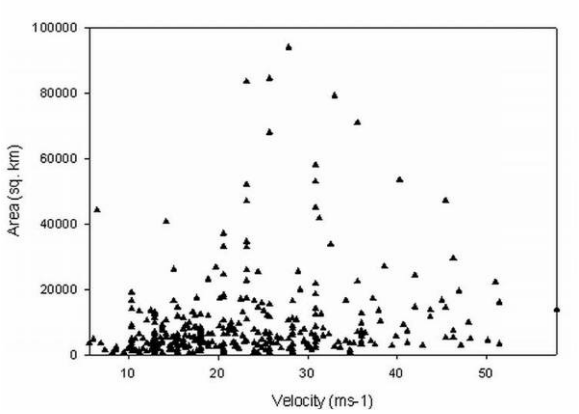

Figure 10. The areas of convective regions according to the maximum sustained wind speed of the TC.

Once a TC is more than 100 km inland, no areas of convection larger than 25,000 km^2 are present (Figure 11). This is likely because less moisture is available over the land surface for latent heat flux (Tuleya, 1994: Kimball, 2008), and continental air masses surrounding the TC have less available moisture to enhance rainfall (Bluestein and Hazen, 1989: Cubukcu et al., 2000). Many of the TCs that remain within 100 km of the coastline post-landfall experience an extratropical transition that helps to increase the area over which convective rainfall occurs. Despite the tendency for inland TCs to have smaller convective rainfall regions, a statistically significant correlation does not exist between a TC's distance from the coastline and the area of its convection (Table 1). When TCs are close to the coastline, areas of strong convection such as those in the eyewalls of hurricanes tend have a limited spatial extent, which accounts for many of the regions that occupy less than 10,000 km^2 visible in Figure 11.

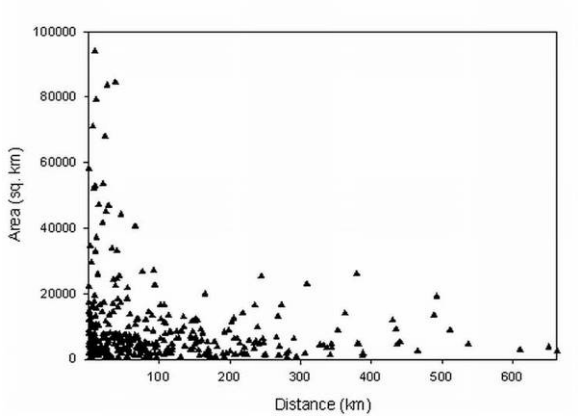

Figure 11. The areas of convective regions according to the distance of the TC circulation center from the coastline.

TCs experiencing vertical wind shear velocities above 10 m s^{-1} have a larger area of convection on average than do TCs experiencing less shear (Figure 12). Nine of the ten largest convective areas for highly-sheared TCs are associated with Floyd (1999) and Bertha (1996) when these TCs were approximately 20-35 hours from becoming extratropical and were located within 50 km of the coastline. Vertical wind shear typically increases during an extratropical transition (Jones, S. C. et al., 2003), and moisture advection from the nearby ocean also contributes to the large area of rainfall associated with these highly-sheared TCs. However, strong vertical wind shear is not solely associated with an extratropical transition, as nearly 40% of the observations for highly-sheared storms occur in TCs that do not become extratropical within 72 hours of landfall. Many of these highly-sheared TCs that do not become extratropical have relatively small areas of convection surrounding their circulation centers as they track inland. Thus, a significant relationship does not exist between the speed of vertical wind shear and the area covered by convection (Table 1).

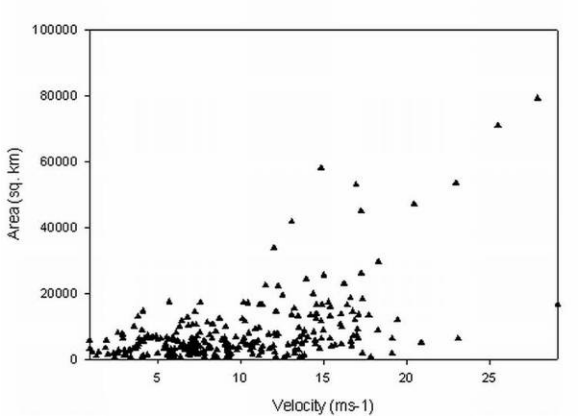

Figure 12. The areas of convective regions according to the velocity of the vertical wind shear.

5. CONCLUSIONS AND FUTURE WORK

This study supports the results of previous modeling and observational studies that suggest convection shifts counterclockwise and spreads outwards from the circulation center of TCs after landfall. Three factors are associated with a counterclockwise shift in convection from the right side to the front of the storm: a) increasing forward velocity, b) decreasing time until extratropical transition, and c) convection forming inland rather than offshore. However, increasing vertical wind shear shifts convection in the clockwise direction. The spreading outwards of convection is associated with a) decreasing storm intensity, b) increasing storm forward velocity, and c) decreasing time until a TC becomes extratropical.

The forward velocity of the TC in conjunction with an extratropical transition had the strongest association with the location of convection both in the radial and azimuthal directions relative to the circulation center of the storm, and also the largest influence on the area over which convection extends. As the forward velocity of TCs increases due to interaction with a middle latitude trough, areas of convection grow in size, are located farther from the circulation center of the storm, and shift counterclockwise from the right side of the storm when motion is slow to the front of the storm when motion is fast. The dynamical changes in the structure of a TC experiencing an extratropical transition act to decrease convection behind and in the core of the storm while increasing convection ahead of the storm so that the same pattern of shifting and growing convection is observed whether examining TCs according to their forward velocity or the time until they become extratropical.

Previous studies suggested that vertical wind shear is the dominant influence on the location of convection within TCs, but the current study found that shear did not have as strong of an association with the location of and area covered by convection as did storm motion and extratropical transition. As found by previous researchers, a clear maximum of convection in the downshear left quadrant convection was observed in the current study. However, a clockwise shift in the region where convection formed from upshear left to downshear right was observed as the velocity of the shear increased, which is a pattern that has not been discussed by previous researchers. Although the areas of convection were larger on average when TCs experienced high shear rather than shear with a velocity less than 10 m s^{-1}, the speed of the vertical wind shear did not significantly alter the radial position of the convection.

This study analyzes a large number of TCs in a GIS framework. To more accurately determine specific locations on the ground that may experience convective rainfall from a TC, and to more effectively link the location of convective rainfall to environmental variables, future work should also utilize the GIS to quantify the shape and orientation of the convective regions. Adding these spatial attributes to the size and location data presented in the current study will allow a complete set of spatial attributes to be cataloged for each convective region. Additional factors that may affect the development and displacement of convection such as the angle at which a TC crosses the coastline, topography, and moisture present within the atmosphere and soil, will also be considered so that these observational results can be compared to modeling studies that examine similar variables. The results of these future analyses could then be utilized to validate the spatial representation of convective rainfall regions produced by dynamical models such as the HWRF (Davis et al., 2008) and GFDL (Marchok et al., 2007), and statistical predictions of TC rainfall produced by models such as R-CLIPER (Marchok et al., 2007), TRaP (Kidder et al., 2005), and PHRaM (Lonfat et al., 2007).

6. NOTE

The full text and additional analyses accompanying this work will appear in the *International Journal of Applied Geospatial Research* (2010, Volume 1, Issue 2).

7. REFERENCES

Anagnostou, E. N., 2004: A convective/stratiform precipitation classification algorithm for volume scanning weather radar observations. *Meteorol. Appl.*, **11,** 291-300.

Atallah, E. H. and L. R. Bosart, 2003: The extratropical transition and precipitation distribution of Hurricane Floyd (1999). *Mon. Wea. Rev.*, **131,** 1063-1081.

Bluestein, H. B. and D. S. Hazen, 1989: Doppler-radar analysis of a tropical cyclone over land - Hurricane Alicia (1983) in Oklahoma. *Mon. Wea. Rev.*, **117,** 2594-2611.

Cecil, D. J., 2007: Satellite-derived rain rates in vertically sheared tropical cyclones. *Geophys. Res. Lett.*, **34,** L02811.

Chen, S. Y. S., J. A. Knaff, and F. D. Marks, 2006: Effects of vertical wind shear and storm motion on tropical cyclone rainfall asymmetries deduced from TRMM. *Mon. Wea. Rev.*, **134,** 3190-3208.

Corbosiero, K. L. and J. Molinari, 2002: The effects of vertical wind shear on the distribution of convection in tropical cyclones. *Mon. Wea. Rev.*, **130,** 2110-2123.

——, 2003: The relationship between storm motion, vertical wind shear, and convective asymmetries in tropical cyclones. *J. Atmos. Sci.,* **60,** 366-376.

Cubukcu, N., R. L. Pfeffer, and D. E. Dietrich, 2000: Simulation of the effects of bathymetry and land-sea contrasts on hurricane development using a coupled ocean-atmosphere model. *J. Atmos. Sci.,* **57,** 481-492.

Davis, C., W. Wang, S. S. Chen, Y. S. Chen, K. Corbosiero, M. DeMaria, J. Dudhia, G. Holland, J. Klemp, J. Michalakes, H. Reeves, R. Rotunno, C. Snyder, and Q. N. Xiao, 2008: Prediction of landfalling hurricanes with the Advanced Hurricane WRF model. *Mon. Wea. Rev.*, **136,** 1990-2005.

DeMaria, M. and J. Kaplan, 1994: A statistical hurricane intensity prediction scheme (SHIPS) for the Atlantic basin. *Weather and Forecasting*, **9,** 209-220.

DeMaria, M., M. Mainelli, L. K. Shay, J. A. Knaff, and J. Kaplan, 2005: Further improvements to the Statistical Hurricane Intensity Prediction Scheme (SHIPS). *Wea. and Forecasting*, **20,** 531-543.

Elsberry, R. L., 2002: Predicting hurricane landfall precipitation: Optimistic and pessimistic views from the symposium on precipitation extremes. *Bull. Amer. Meteor. Soc.*, **83,** 1333-1339.

Frank, W. M. and E. A. Ritchie, 1999: Effects of environmental flow upon tropical cyclone structure. *Mon. Wea. Rev.*, **127,** 2044-2061.

Geerts, B., G. M. Heymsfield, L. Tian, J. B. Halverson, A. Guillory, and M. I. Mejia, 2000: Hurricane Georges's landfall in the Dominican Republic: Detailed airborne Doppler radar imagery. *Bull. Amer. Meteor. Soc.*, **81,** 999-1018.

Jones, R. W., 1987: A simulation of hurricane landfall with a numerical-model featuring latent heating by the resolvable scales. *Mon. Wea. Rev.*, **115,** 2279-2297.

Jones, S. C., P. A. Harr, J. Abraham, L. F. Bosart, P. J. Bowyer, J. L. Evans, D. E. Hanley, B. N. Hanstrum, R. E. Hart, F. Lalaurette, M. R. Sinclair, R. K. Smith, and C. Thorncroft, 2003: The extratropical transition of tropical cyclones: Forecast challenges, current understanding, and future directions. *Wea. and Forecasting*, **18,** 1052-1092.

Jorgensen, D. P., 1984: Mesoscale and convective-scale characteristics of mature hurricanes. Part I: General observations by research aircraft. *J. Atmos. Sci.,* **41,** 1268-1285.

Kidder, S. Q., S. J. Kusselson, J. A. Knaff, R. R. Ferraro, R. J. Kuligowski, and M. Turk, 2005: The tropical rainfall potential (TRaP) technique. Part I: Description and examples. *Wea. and Forecasting*, **20,** 456-464.

Kimball, S. K., 2008: Structure and evolution of rainfall in numerically simulated landfalling hurricanes. *Mon. Wea. Rev.*, **136,** 3822-3847.

Lawrence, M. B., L. A. Avila, J. L. Beven, J. L. Franklin, J. L. Guiney, and R. J. Pasch, 2001: Atlantic hurricane season of 1999. *Mon. Wea. Rev.*, **129,** 3057-3084.

Lonfat, M., F. D. Marks, and S. Y. S. Chen, 2004: Precipitation distribution in tropical cyclones using the Tropical Rainfall Measuring Mission (TRMM) Microwave

Imager: A global perspective. *Mon. Wea. Rev.*, **132,** 1645-1660.

Lonfat, M., R. Rogers, T. Marchok, and F. D. Marks, 2007: A parametric model for predicting hurricane rainfall. *Mon. Wea. Rev.*, **135,** 3086-3097.

Marchok, T., R. Rogers, and R. Tuleya, 2007: Validation schemes for tropical cyclone quantitative precipitation forecasts: evaluation of operational models for US Landfalling cases. *Wea. and Forecasting*, **22,** 726-746.

Molinari, J., P. Moore, and V. Idone, 1999: Convective structure of hurricanes as revealed by lightning locations. *Mon. Wea. Rev.*, **127,** 520-534.

NHC, 2006. Official Record of Hurricanes and Tropical Storms in the Atlantic Basin. Available at www.aoml.noaa.gov/hrd/Data_Storm.html.

Powell, M. D., 1990: Boundary-layer structure and dynamics in outer hurricane rainbands .1. Mesoscale rainfall and kinematic structure. *Mon. Wea. Rev.*, **118,** 891-917.

Rappaport, E. N., 2000: Loss of life in the United States associated with recent Atlantic tropical cyclones. *Bull. Amer. Meteor. Soc.*, **81,** 2065-2073.

Shapiro, L. J., 1983: The asymmetric boundary-layer flow under a translating hurricane. *J. Atmos. Sci.,* **40,** 1984-1998.

Shepherd, J. M., A. Grundstein, and T. L. Mote, 2007: Quantifying the contribution of tropical cyclones to extreme rainfall along the coastal southeastern United States. *Geophys. Res. Lett.s*, **34,** 5.

Tuleya, R. E., 1994: Tropical storm development and decay: Sensitivity to surface boundary-conditions. *Mon. Wea. Rev.*, **122,** 291-304.

Wilks, D. S., 1995: *Statistical Methods in the Atmospheric Sciences*. Academic Press, 467 pp.

Willoughby, H. E., F. D. Marks, and R. J. Feinberg, 1984: Stationary and moving convective bands in hurricanes. *J. Atmos. Sci.,* **41,** 3189 - 3211.